Poisoning of Pt 3 Co Electrodes: A Combined Experimental and DFT Study

ARTICLE *in* THE JOURNAL OF PHYSICAL CHEMISTRY C · MAY 2010

Impact Factor: 4.77 · DOI: 10.1021/jp906778k

4 AUTHORS, INCLUDING:

M. D. Johannes
United States Naval Research Laboratory
94 PUBLICATIONS **3,614** CITATIONS
SEE PROFILE

Yannick Garsany
United States Naval Research Laboratory
35 PUBLICATIONS **548** CITATIONS
SEE PROFILE

Karen E. Swider-Lyons
United States Naval Research Laboratory
105 PUBLICATIONS **1,526** CITATIONS
SEE PROFILE

Langmuir

ARTICLE

pubs.acs.org/Langmuir

Products of SO_2 Adsorption on Fuel Cell Electrocatalysts by Combination of Sulfur K-Edge XANES and Electrochemistry

Olga A. Baturina,*[,†] Benjamin D. Gould,[†] Anna Korovina,[†] Yannick Garsany,[‡] Richard Stroman,[†] and Paul A. Northrup[§]

[†]Chemistry Division, Naval Research Laboratory, Washington, DC 20375, United States

[‡]EXCET Inc., Springfield, Virginia 22151, United States

[§]Stony Brook University, Stony Brook, New York 11794, United States

ABSTRACT: Electrochemical adsorption of SO_2 on platinum is complicated by the change in sulfur oxidation state with potential. Here, we attempt to identify SO_2 adsorption products on catalyst coated membranes (CCMs) at different electrode potentials using a combination of *in situ* sulfur K-edge XANES (X-ray absorption near-edge structure) spectroscopy and electrochemical techniques. CCMs employed platinum nanoparticles supported on Vulcan carbon (Pt/VC). SO_2 was adsorbed from a SO_2/N_2 gas mixture while holding the Pt/VC-electrode potential at 0.1, 0.5, 0.7, and 0.9 V vs a reversible hydrogen electrode (RHE). Sulfur adatoms (S^0) are identified as the SO_2 adsorption products at 0.1 V, while mixtures of S^0, SO_2, and sulfate/bisulfate ((bi)sulfate) ions are suggested as SO_2 adsorption products at 0.5 and 0.7 V. At 0.9 V, SO_2 is completely oxidized to (bi)sulfate ions. The identity of adsorbed SO_2 species on Pt/VC catalysts at different electrode potentials is confirmed by modeling of XANES spectra using FEFF8 and a linear combination of experimental spectra from sulfur standards. Results on SO_2 speciation gained from XANES are used to compare platinum−sulfur electronic interactions for Pt_3Co/VC versus Pt/VC catalysts in order to understand the difference between the two catalysts in terms of SO_2 contamination.

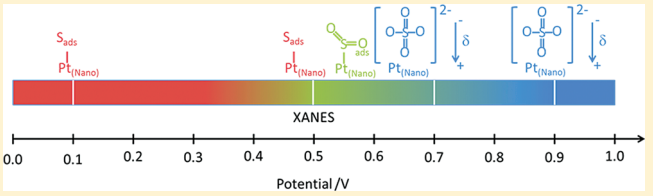

INTRODUCTION

Sulfur dioxide is a common air impurity that can severely poison the platinum catalyst used in commercial proton exchange membrane fuel cells (PEMFCs). The extent of poisoning depends on fuel cell (FC) operating voltage[1] because the nature and oxidation state of SO_2 adsorption products are functions of electrode potential.[2−8] Speciation of adsorbed SO_2 species on platinum has been a subject of thorough investigations.[2−8] However, these studies were mostly focused on polycrystalline platinum or platinum thin films at the electrode/solution interface. Fewer papers have addressed SO_2 speciation on Pt nanoparticles.[1,9,10] Latter studies were mostly performed in PEMFCs, as commercial fuel cell catalysts employ platinum nanoparticles supported on VC. The results of SO_2 adsorption experiments conducted in H_2|air (anode|cathode) and $H_2|N_2$ cells suggest that sulfur adatoms (S^0) are the products of SO_2 adsorption at 0.5 V, a mixture of SO_2 and (bi)sulfate ions is generated at 0.6−0.8 V, and (bi)sulfate ions are produced at 0.9 V.[1,9]

In order to elucidate the nature of adsorbed species, electrochemical techniques are usually combined with *in situ* spectroscopy to provide molecular level information about the identity and structure of adsorbed species. Examples of such previously used techniques are *in situ* Fourier-transformed infrared (FTIR) and surface-enhanced Raman spectroscopy (SERS).[8,11] These techniques have been used to determine the oxidation state of SO_2 on platinum in an aqueous solution of 0.5 M H_2SO_4. Wilke et al.[8] used voltammetry coupled with SERS to determine SO_2 adsorption products on thin platinum films (2−3 monolayers) electrodeposited on gold. Voltammetric response indicated that SO_2 was oxidized at potentials more positive than 0.64 V versus normal hydrogen electrode (NHE) and reduced at potentials more negative than 0.14 V. The spectroscopic response was different: SO_2 was stable to oxidation and reduction for electrodes held at 0.14−0.24 V, while it was oxidized and reduced at potentials more positive than 0.44 V and negative than 0.14 V, respectively. The reduction product was assigned to atomic sulfur, while the oxidation products were assigned to SO_3 and/or sulfate. Molecular SO_2 was observed on the surface along with SO_3 and/or sulfate at 0.44−0.94 V.

Quijada et al.[11,12] studied SO_2 oxidation and reduction on polycrystalline platinum by cyclic voltammetry (CV) combined with FTIR. SO_2 oxidation was observed at potentials more positive than 0.65 V, while it was reduced at potentials more negative than 0.65 V. (Bi)sulfate ions were found to be the only stable oxidation products at 0.65−1.4 V. The presence of molecular SO_2 could not be clearly identified in this potential region, as its IR peak was weak and inconclusive. SO_2 reduction products in the potential region of 0.65−0.1 V were IR-inactive, which allowed the authors to rule out H_2S/HS^-, dithionite, and

Received: August 25, 2011
Revised: October 26, 2011
Published: November 02, 2011

thiosulphate ions as possible reduction products. Atomic sulfur and a mixture of atomic sulfur with polysulfide species were suggested as the ultimate SO_2 reduction products for potential regions of 0.65−0.2 V, and 0.2−0 V, respectively. This assignment was made on the basis of voltammetric response and visual inspection of the electrodes after exposure to reduction potentials.

It should be noted that the interpretation of the *in situ* SERS[8] and FTIR[11,12] results on the speciation of adsorbed SO_2 species on platinum at the electrode/solution interface was not unambiguous, as it was complicated by difficulties with identification of multiple peaks of sulfur compounds[8] or IR-inactivity of SO_2 adsorption products.[11,12]

Here we report our results on the speciation of adsorbed SO_2 species as a function of electrode potential on commercial FC electrodes employing Pt/VC catalysts. SO_2 adsorption in such electrodes occurs on platinum nanoparticles at the triple phase boundary, contrary to previous studies in which SO_2 was adsorbed either on electrodeposited thin (2−3 monolayers) films of platinum on gold[8] or on polycrystalline platinum[11,12] at the electrode/solution interface. Unlike polycrystalline platinum or platinum thin films, platinum nanoparticles have corner and edge sites that can significantly change their reactivity toward SO_2 oxidation/reduction.[13,14] Platinum nanoparticles are surrounded by Nafion ionomer in the catalyst layers of the CCMs, meaning that there is an additional barrier for the SO_2 species on the way to the surface of the platinum nanoparticles.

We use *in situ* sulfur K-edge XANES spectroscopy in order to get direct information on the nature of adsorbed SO_2 species on FC electrodes at different electrode potentials. The sulfur K-edge XANES is a powerful tool to distinguish between sulfur species in different oxidation states because of the significant shift (ca. 10 eV) in XANES peak-energy positions for zerovalent sulfur (S^0) and sulfate species (S^{6+}).[15] However, measurements at the low energy of the sulfur K-edge (ca. 2480 eV) require use of a specialized beamline and particular attention to experimental design. This is the first attempt to identify adsorbed SO_2 species on Pt nanoparticles as a function of electrode potentials using *in situ* sulfur K-edge XANES.

X-ray absorption spectroscopy at the higher energy Pt L_3 edge (ca. 11.5 keV) has recently been used by Ramaker et al.[14] to resolve the effect of SO_2 on Pt/VC catalysts. SO_2 species were adsorbed on the Pt surface *ex situ* from a Na_2SO_3 aqueous solution, and *in situ* spectroscopic response of Pt to applied potential was monitored. The SO_2 effect was inferred. In our experiments, the SO_2 effect is directly demonstrated using sulfur K-edge XANES.

SO_2 adsorption on Pt/VC catalysts was performed from a SO_2/N_2 mixture flowing through the working electrode (WE) compartment while the WE potential was held at 0.1−0.9 V versus reversible hydrogen electrode (RHE). The potential range goes beyond the typical fuel cell operation region 0.5−0.7 V to cover a broader range of conditions that the fuel cell can experience. The identity of SO_2 adsorption products as a function of electrode potential was determined from comparison with sulfur standards and verified by FEFF8[16] and combination fit[15,17] modeling. To the best of our knowledge, for the first time several adsorbed species are simultaneously and unambiguously identified on the surface of Pt nanoparticles incorporated into the structure of the CCMs.

Information on sulfur speciation on Pt/VC catalysts gained from XANES was used to compare Pt_3Co/VC versus Pt/VC catalysts with respect to SO_2 contamination as a follow up to our group's prior RDE,[18,19] theoretical,[20] and fuel cell[18] work.

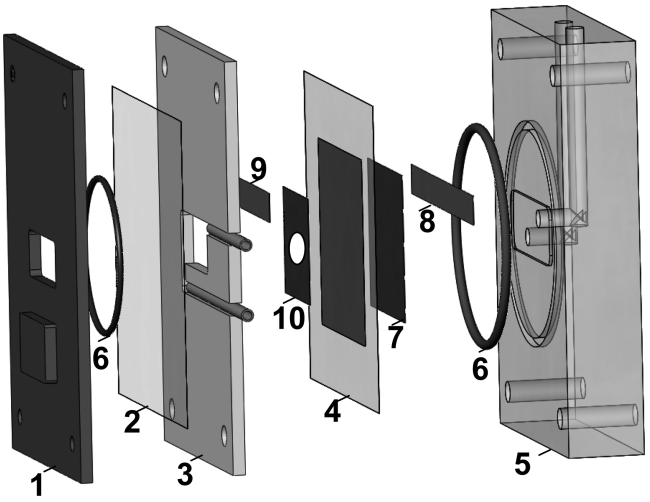

Figure 1. Exploded view of the cell for *in situ* spectroelectrochemical measurements at X15B. The cell assembly includes a stainless steel front plate (1), 5 μm polypropylene film (2), polycarbonate gas manifold (3), CCM (4), polycarbonate back plate (5), Viton o-rings (6), carbon cloth (7 and 10), platinum counter electrode (8), and gold WE lead (9).

EXPERIMENTAL SECTION

XANES Samples. The two representative FC catalysts used in these studies were Pt/VC and Pt_3Co/VC. The Pt/VC was purchased as CCMs from Ion Power, Inc. A CCM consisted of catalyst layers containing 50 wt % Pt/VC catalyst and Nafion ionomer deposited on both sides of a NRE 212 membrane (DuPont). The platinum loading was 0.4 mg_{Pt} cm^{-2} at the cathode|anode, and the catalyst-coated surface areas were 10 cm^2. The Pt_3Co/VC CCMs were custom-made by Ion Power, Inc., using a 30 wt % (total metal loading) Pt_3Co/VC catalyst (BASF, developmental) and Nafion ionomer at the cathode. The Pt loading of the Pt_3Co/VC cathodes was 0.4 mg_{Pt} cm^{-2}.

$CuFeS_2$ (S^{2-}), elemental sulfur S_8 (S^0), sodium sulfite (S^{4+}), and a natural calcite ($CaCO_3$) mineral sample containing dilute sulfate (S^{6+}) were all used as standards to calibrate the sulfur K-edge energies. Elemental sulfur and sodium sulfite (Sigma Aldrich, ACS grade) were diluted to 0.3 wt % sulfur by grinding in mixture with boron nitride powder (Sigma Aldrich, ACS grade). This minimized the self-absorption during X-ray absorption measurements in fluorescence mode.[15] The peak position for elemental sulfur was set to 2472.4 eV during the instrument calibration. Powders of standards were finely ground and placed into 5 mm ×8 mm envelopes made of 5 μm thick polypropylene film (SPEXCertiPrep, Inc.) for collection of XANES spectra.

XANES Cell. A custom *in situ* electrochemical flow cell was fabricated to allow for low-energy XANES measurements while the working electrode (WE) was under potential control. Figure 1 shows a solid model rendering of the cell. The *in situ* electrochemical cell was based on previous designs.[21] However, the cell was modified to allow for measurements in a fluorescence mode and to incorporate gaseous flow. The cell consisted of a sandwich of the following pieces, listed in order of beam incidence: stainless steel front plate (1) with window frame, a 5 μm film (2) of polypropylene (SPEXCertiPrep, Inc.), polycarbonate miniature gas manifold (3), CCM (4), and polycarbonate back plate (5) with a "no leak" Ag/AgCl reference electrode (Cypress Systems, Inc.). Our innovation versus previous designs was in incorporating the gas manifold (3) to allow for measurements in the gaseous flow. The cell was sealed by

compressing Viton o-rings (6) between the catalyst assembly and the back plate (5), and between the front plate (1) and the gas manifold (3). The threaded front plate (1) was screwed hand tight to the back plate (5) using 4 hex screws.

The cell was assembled in a horizontal orientation by placing an E-TEK carbon cloth (7) soaked in 1.0 M $HClO_4$ on top of the polycarbonate back plate (5). A platinum counter electrode (8) was placed on top of the carbon cloth (7) followed by the fuel cell CCM (4) on top of the carbon cloth (7) with the cathode side up (facing beam path). A working electrode (WE) lead made of gold foil (9) was placed in direct contact with the cathode catalyst side. A carbon cloth (10) with a 6 mm diameter hole was soaked in 0.1 M HBF_4 and placed on top of the gold WE lead (9). The counter electrode (8), WE lead (9), CCM (4), and carbon cloths (7, 10) formed the fuel cell catalyst assembly. The gas manifold (3) was placed on top of the fuel cell catalyst assembly. The beam window material (2) and the front plate (1) were placed on top of the gas manifold (3). The entire sandwich was compressed together and placed in the vertical position. The cavity in the back plate was filled with 1.0 M $HClO_4$, and the Ag/AgCl reference electrode was placed in the longest hole. Care was taken to exclude bubbles from the reference electrode channel.

The cell was then mounted to a sample holder in the beamline hutch. Electrical leads and gas feeds were connected to the cell.

Aqueous solutions of 1.0 M $HClO_4$ and 0.1 M HBF_4 used in the spectroelectrochemical cell were prepared by dilution of double-distilled $HClO_4$ (70 wt % GFS Chemicals) and 50 wt % HBF_4 (Acros Organics) with 18 MΩ cm nanopure water (Millipore).

Collection of XANES Spectra. The sulfur K-edge XANES spectra were measured using the X15B beamline at the National Synchrotron Light Source (NSLS) of Brookhaven National Lab. The beam was focused to a 1 mm^2 spot size at the sample. X15B was equipped with a Si(111) monochromator, with an energy resolution of 0.35 eV at the sulfur K-edge. The XANES spectra were acquired in fluorescence mode using a Canberra germanium solid-state detector cooled by liquid nitrogen and positioned 90° to the incident beam. The sulfur K-edge fluorescence was isolated from the detector spectrum. Incident beam intensity (I_0) was measured using a windowless ionization chamber. The entire sample environment was purged to helium at 1 atm. More details on X15B beamline can be found on the NSLS website.[22]

The spectra for both sulfur standards and adsorbed SO_2 species on platinum catalysts in the electrochemical cell were collected by scanning incident energy from 2420 to 2560 eV, with a step size of 2 and 1 eV below 2460 and above 2560 eV, respectively. The step sizes across the edge (2460−2525 eV) were smaller: 0.25 eV between 2460 and 2490 eV and 0.5 eV between 2490 and 2525 eV. The acquisition time was 8 s for points between 2460 and 2525 eV and 4 s everywhere else.

***In-Situ* XANES Spectroelectrochemical Cell.** Once the cell was placed in the hutch, the hutch was purged with He until the incident beam intensity (I_0) became stable. In the meantime the WE compartment of the cell was purged with humidified research grade nitrogen (N_2 6.0, GTS-Welco). The N_2 was humidified by passing it through a glass frit bubbler filled with approximately 200 mL of 0.1 M HBF_4. During the N_2 flush, a baseline XANES spectrum was acquired to ensure that everything was working properly and that the catalyst surface was free of any sulfur species. Once the baseline spectrum was complete, the cell was then placed under potential control using a PGSAT30 AutoLab potentiostat, and a steady state electrochemical current was recorded for 5 min. After the steady state electrochemical current was acquired, 1000 ppm SO_2 in research grade N_2 (GTS-Welco) was fed into the cell, and the SO_2 oxidation/reduction current was monitored. After 15 min, the flow of SO_2/N_2 was ceased, and the cell was flushed with humidified N_2 for 10 min to remove any gaseous SO_2 that would obscure the sulfur surface species during XANES. XANES spectra of the catalyst layer after SO_2 exposure were recorded under flowing N_2. After recording the XANES spectra, the Pt-surface was stripped of sulfur species through 10 CV sweeps using the following polarization program: hold potential → 0.05 V → 1.4 V → 0.05 V versus RHE. A final XANES spectrum was recorded at the end to ensure that all sulfur species were oxidatively desorbed from the platinum surface.

Treatment of the Experimental XANES Spectra. The experimental XANES spectra were recorded as relative intensity ($I_{fluorescence}/I_0$) as a function of photon energy. For further analysis, the spectra were linear pre-edge background corrected (by subtraction of linear pre-edge background) and normalized to a postedge step height of unity (if it was necessary for the purpose of their comparison).

Experimental XANES spectra measured after exposure to 1000 ppm SO_2 in N_2 at 0.1, 0.5, and 0.7 V were fitted as a linear combination of single spectra[15,17] for the S^0, S^{4+}, S^{6+} standards and S^{5+} from the Nafion sulfonic group. The spectrum of the S^0 standard was shifted by −0.8 eV along the energy axis for fitting performed at 0.1 V and by −1.3 eV for fitting performed at 0.5 and 0.7 V. Similarly, the spectrum of the S^{4+} standard was shifted by −2 eV. This shifting accounts for the electron donation from platinum to sulfur adsorbed species. The "Dynamic Fit Wizard" provided by SigmaPlot 10 software was used to fit the best combination of spectra. The fitting software is based on the Marquardt−Levenberg algorithm[23] that finds parameters providing the best fit between experimental and simulated curves. In our particular case this algorithm was used to find the best fit between each experimental XANES spectrum obtained after exposure to 1000 ppm SO_2 in N_2 at a given potential and the one calculated by the equation below:

$$Y = A\bullet\{S^0\} + B\bullet\{S^{4+}\} + C\bullet\{S^{5+}\} + D\bullet\{S^{6+}\} \quad (1)$$

Here A, B, C, and D are the fractions of individual spectra for S^0, S^{4+}, S^{5+}, and S^{6+} in the total spectrum Y. For simplicity, it was assumed that A + B + C + D = 1. Before performing the fitting procedure, both experimental spectra and sulfur standards spectra were pre-edge background-corrected and normalized to a postedge step height of unity.

Modeling of XANES Spectra for Solid Standards and Adsorbed SO_x Species (x = 0, 2, and 4) on Pt Clusters. Theoretical sulfur K-edge XANES spectra were calculated for two types of sulfur clusters in varying sulfur oxidation state using FEFF8.[24] The first set of calculations considered S_8 (S^0), Na_2SO_3 (S^{4+}), and Na_2SO_4 (S^{6+}) sulfur clusters as the bulk. The binding geometry for each cluster was obtained from the literature.[25−28] The second set of calculations considered S^0, SO_2, and SO_4^{2-} species as an adsorbate on a model Pt Janin[29] cluster. The Janin[29] cluster is preferred because it contains both fcc and hcp sites and, due to the lower cluster symmetry (compared to highly symmetric octahedral cluster[16,30,31]), a problematic surface state near the Fermi level does not arise. A Janin Pt_6 cluster was utilized with a Pt−Pt distance of 2.77 Å to carry out the FEFF8 results. The adsorbate cluster geometry was obtained from the work of Lin et al.[32,33] who performed theoretical calculations using DFT on SO_x (x = 0, 2, and 3) species adsorbed on Pt(111) surfaces to determine the most thermodynamically stable orientation and geometric binding site for the S species. The binding geometry for SO_2 in an $\eta^2S_bO_a$ site, SO_3 in an $\eta^3S_aO_aO_a$ site, and SO_4 in $\eta^1O_f(SO_3)_f$ orientation was used,[32,34] where η refers to the number of atoms bound to the Pt surface and the subscripts "a", "b", and "f" refer to atop, bridged, and 3-fold fcc sites, respectively.

RESULTS AND DISCUSSION

Standards. Figure 2 shows the sulfur K-edge XANES spectra of the different sulfur standards and a Nafion 212 membrane after pre-edge background correction and step height normalization to unity. These spectra were used to assign the sulfur oxidation state of SO_2 adsorption products in the *in situ* spectroelectrochemical experiments. The standards include solid $CuFeS_2$ (S^{2-}, red), elemental sulfur (S^0, black), Na_2SO_3 (S^{4+}, green), and dilute

sulfate in $CaCO_3$ (S^{6+}, dark cyan). Nafion is not considered as a standard here because the sulfur oxidation state in sulfur organic compounds or polymers is often different from the oxidation state predicted by conventional rules.[35] The spectrum measured for the Nafion 212 membrane is shown in Figure 2 as a dashed blue line.

Each spectrum in Figure 2 is characterized by a strong sharp peak corresponding to an absorption edge maximum. In agreement with the results of previous studies,[17,35,36] the absorption edge energy is directly related to the oxidation state of sulfur, with more positive photon energies of the absorption edge maxima corresponding to higher sulfur oxidation states. The intensity of the absorption edge maxima increases with increasing sulfur oxidation state due to the increase in the photoabsorption cross section.[17,37,38]

The positions of the absorption edge maxima for all the sulfur standards are given in Table 1. Peak energy positions as a function of sulfur oxidation states are shown as an inset in Figure 2. They fall on a straight line that can be used as a calibration plot to determine the sulfur oxidation state in polymer compounds such as Nafion. Using this calibration plot, the sulfur oxidation state in the Nafion sulfonic group should be assigned to 5+, not the conventional oxidation state of 4+ in Na_2SO_3. A sulfur oxidation state of 5+ in the Nafion sulfonic group seems reasonable, considering that, unlike the sulfonic group in sodium sulfite, the sulfur atom in the Nafion sulfonic group is bound not only to more electronegative oxygen atoms, but also to a carbon atom.[39] As both sulfur and carbon have the same electronegativities, covalent bonding with carbon should not result in changing the sulfur oxidation state.[35] The difference between sulfur oxidation states defined by conventional rules and determined by XANES have been analyzed previously by Vairavamurthy[35] for different groups of sulfur organic compounds.

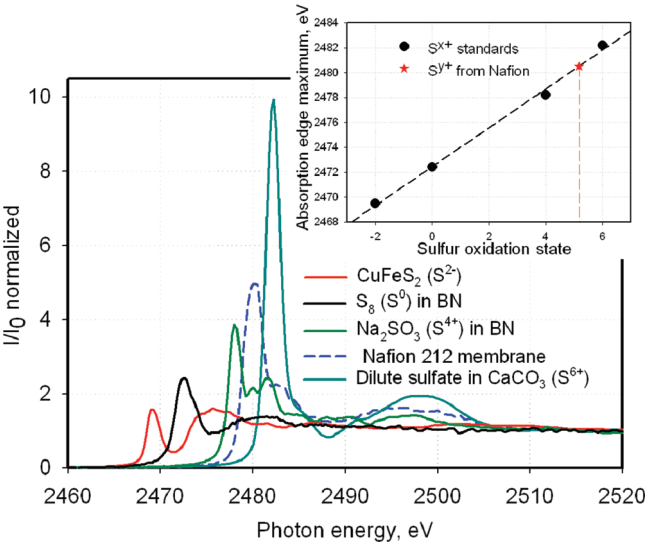

Figure 2. Pre-edge background corrected XANES spectra of $CuFeS_2$ (red), elemental sulfur S_8 (black), Na_2SO_3 (green), dilute sulfate in $CaCO_3$ (cyan), and the Nafion 212 film (blue dashed line).

Current (I) versus Time Curves during WE Exposure to 1000 ppm SO_2 in Nitrogen at 0.1−0.9 V. Figure 3 shows background-corrected currents (I_{corr}) versus time curves recorded before, during, and after exposure of the WE to 1000 ppm SO_2 in N_2 for 15 min while holding the WE potentials at 0.1, 0.5, 0.7, and 0.9 V. I_{corr} values were calculated by subtracting the currents measured in the presence of SO_2 from currents measured in blank experiments, when the WE was held at different potentials in the presence of humidified nitrogen. As the holding potential becomes more positive, SO_2 reduction at 0.1 V (black line) changes to SO_2 oxidation at 0.7 and 0.9 V (blue and purple lines, respectively). In all three experiments, the currents reach steady values within the first minute of exposure to SO_2 in N_2. The steady-state SO_2 oxidation current increases with potential, in qualitative agreement with the results of Spotnitz et al.[40] At 0.5 V, the shape of the current versus time curve (red line) differs from the other three experiments. The reduction current increases for the first 30 s and then gradually approaches zero. This is likely due to the fact that SO_2 reduction occurs in parallel to SO_2 adsorption, and adsorbed molecules eventually completely suppress the reduction process. When the SO_2/N_2 flow is replaced by the N_2 flow, the background-corrected currents drop to zero inferring that SO_2 reduction/oxidation has ceased.

XANES Spectra after WE Exposure to 1000 ppm SO_2 in N_2 at 0.1−0.7 V. Figure 4 compares the pre-edge background corrected XANES spectra recorded for the WE held at 0.1 V (a), 0.5 V (b) and 0.7 V (c) in the spectroelectrochemical cell after exposure to SO_2/N_2 followed by a 10 min purge with humidified N_2. The peak positions are given in Table 2. The dotted lines in Figure 4a−c are the background spectra recorded before exposure of the WEs to a SO_2/N_2 flow. The only feature of the background spectra is a sharp peak at 2480.5 ± 0.1 eV due to the presence of sulfur in the sulfonic group of the Nafion ionomer (see the peak position of Nafion 212 in Table 1). In spite of the fact that Vulcan carbon may contain up to 0.5 wt % of sulfur,[41] no sulfur peaks are detected in the range 2470−2478 eV. This implies that interference from sulfur signals associated with carbon is not an issue for high-loaded carbon-supported platinum catalysts. Therefore, the sulfur K-edge XANES can be

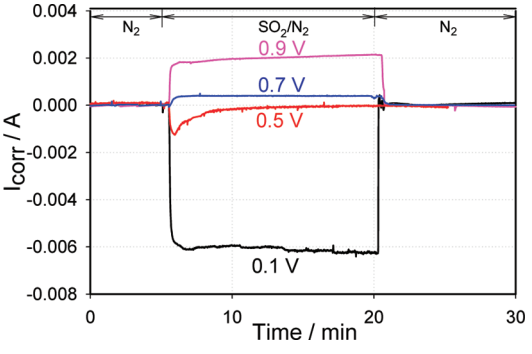

Figure 3. I_{corr} vs time curves recorded before, during, and after exposure of the Pt/VC electrode held at 0.1−0.9 V to 1000 ppm SO_2 in N_2. The WE chamber was purged with research grade N_2 for 5 and 10 min before and after exposure to SO_2, respectively.

Table 1. Photon Energies Corresponding to the Absorption Edge Maxima on XANES Spectra of Sulfur Standards and Nafion 212 Membrane

sulfur compound:	$CuFeS_2$ (S^{2-})	S_8 (S^0)	Na_2SO_3 (S^{4+})	dilute $CaSO_4$ in $CaCO_3$ (S^{6+})	Nafion 212 membrane
photon energy, ±0.2 eV:	2469.5	2472.4	2478.2	2482.2	2480.5

dx.doi.org/10.1021/la2033466 |Langmuir 2011, 27, 14930–14939

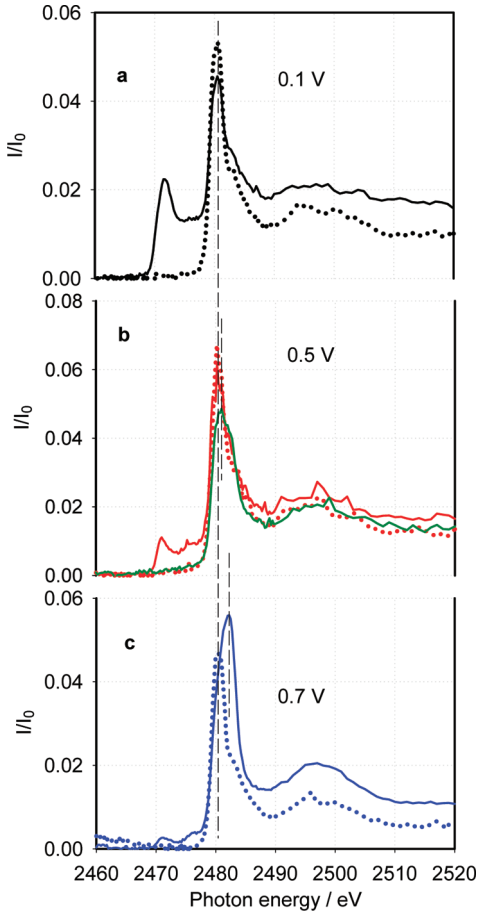

Figure 4. Pre-edge background corrected XANES spectra measured before (···) and after (—) carrying out potentiostatic experiments depicted in Figure 3 while holding the WE at 0.1 (a), 0.5 (b), and 0.7 V (c). Also shown, XANES spectrum recorded after running eight CV curves (green curve in Figure 4b). The peak positions for each spectrum are given in Table 2.

used for studying the platinum−sulfur interactions in such catalysts.

The solid black curve in Figure 4 a is a spectrum obtained after exposure of the WE to SO_2/N_2 while holding its potential at 0.1 V. In addition to a peak at 2480.5 ± 0.1 eV that was observed on the background spectrum, a well-defined peak at 2471.6 ± 0.1 eV is measured. This peak can be assigned to the reduction product of SO_2 consistent with the reduction current observed during exposure of the WE to a SO_2/N_2 mixture at 0.1 V (see black curve in Figure 3). The position of this peak is 0.8 eV more negative than the peak position for the S^0 standard (2472.4 ± 0.1 eV, Table 1). The negative shift is likely due to electron donation from platinum to sulfur. This shift is not large enough to suggest the formation of an ionic Pt−S bond or platinum sulfide. An ionic Pt−S bond would require an energy difference of ∼2.9 eV, similar to the difference observed for the peaks of elemental sulfur (S^0) versus $CuFeS_2$ (S^{2-}) (Table 1).

When the WE potential is held at 0.5 V (red solid line in Figure.4b) during SO_2 exposure, the intensity of the peak observed at 2471.6 ± 0.1 eV decreases while its position shifts negatively by 0.6 ± 0.1 eV. In addition, one smaller peak appears at 2476 ± 0.2 eV. The position of the peak at 2480.4 ± 0.1 eV remains unchanged. When the contamination experiments are carried on the WE held at 0.7 V (blue solid line in Figure 4c), the positions of the two lower energy peaks (2471 ± 0.1 eV and 2476.2 ± 0.2 eV) do not change, while their intensities decrease and the peak at 2476.2 ± 0.2 eV becomes more pronounced than the peak at 2471 ± 0.1 eV, meaning that the fraction of the former product decreases with respect to the fraction of the latter product. Interestingly, the peak observed previously at 2480.5 eV shifts positively to 2482.1 ± 0.1 eV, and its intensity increases versus the intensity of the respective peak on the background spectrum. The spectrum shown by green solid line in Figure 4b will be discussed later.

Table 2. Peak Positions from XANES Spectra Recorded after the Exposure of the Pt/VC-Based Electrodes to 1000 ppm SO_2/N_2 at 0.1, 0.5, and 0.7 V

	clean CCM	0.1 V	0.5 V	0.7 V
1st peak, ±0.2 eV		2471.6	2471.0	2471.1
2nd peak, ±0.2 eV			2476.0	2476.2
3rd peak, ±0.2 eV	2480.5	2480.5	2480.4	2482.1

We assign the peaks at 2471.0 ± 0.1 eV and 2476 ± 0.2 eV in Figure 4b,c to adsorbed sulfur (S^0) and SO_2, respectively, even though both of them are shifted negatively with respect to their standards (see Table 1). Similar to Figure 4a, negative shifting is likely due to some additional negative charge residing on the sulfur atoms, as both sulfur adatoms and SO_2 species are adsorbed on a platinum surface, with the sulfur atoms being directly exposed to a platinum surface. The shift in energy of the peak observed at 2480.5 ± 0.1 eV coupled with an increase in its intensity upon switching from 0.1 V (Figure 4a) and 0.5 V (Figure 4b) to 0.7 V (Figure 4c) can be unambiguously assigned to generation of (bi)sulfate ions on the platinum surface. Unlike the peaks for S^0 and SO_2, the peak for the S^{6+} standard (dilute $CaSO_4$ in $CaCO_3$) closely matches the experimentally observed peak at 2482.1 ± 0.1 eV (Table 2). Such good agreement between the peak positions for (bi)sulfate ions on the platinum surface (2482.1 ± 0.1 eV) and S^{6+} standard (2482.2 ± 0.1 eV, Table 1) is likely due to the fact that the sulfur atoms in (bi)sulfate ions are surrounded by a tetrahedron of oxygen atoms[42,43] and not exposed directly to platinum atoms on the surface.

(Bi)sulfate generation on the platinum surface identified by XANES is consistent with the oxidation current on the I_{corr} versus time curve observed during exposure of the Pt/VC catalyst to SO_2/N_2 at 0.7 V (blue curve in Figure 3). Figure 5 shows an overlay of the XANES spectra obtained after exposure of the working electrodes to SO_2/N_2 at 0.1, 0.5, and 0.7 V.

A XANES spectrum was also collected after exposure to SO_2/N_2 of the WE held at 0.9 V. This spectrum is not shown in Figures 4 and 5 because the dosage of SO_2 was lower versus the other three experiments. However, the shape of the spectrum at 2480−2482 eV suggested enhanced (bi)sulfate generation after the WE exposure to SO_2/N_2.

Simulated XANES Spectra for SO_x Adsorbed Species ($x = 0$, 2, and 4) on Pt Clusters versus Solid Standards (S, Na_2SO_3, and Na_2SO_4). To get a better understanding of the influence of platinum-adsorbate interaction on the shape and peak positions of the XANES spectra, simulated spectra for SO_x species adsorbed on a Pt_6 Janin cluster[29] were compared to that of clusters representing solid standards of elemental sulfur S_8 (cyclooctasulfur[44]), Na_2SO_3, and Na_2SO_4 in Figure 6 a,b, respectively. The theory describes well some features of experimental spectra of solid

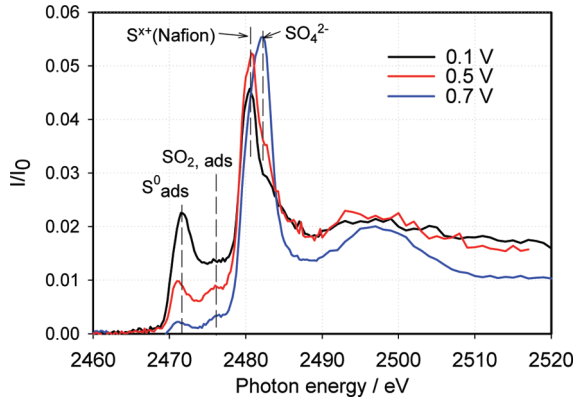

Figure 5. Pre-edge background corrected XANES spectra measured after carrying out potentiostatic experiments depicted in Figure 3 while holding the WE at 0.1 (black), 0.5 (red), and 0.7 (blue) V. Also shown in Figure 4a−c (—).

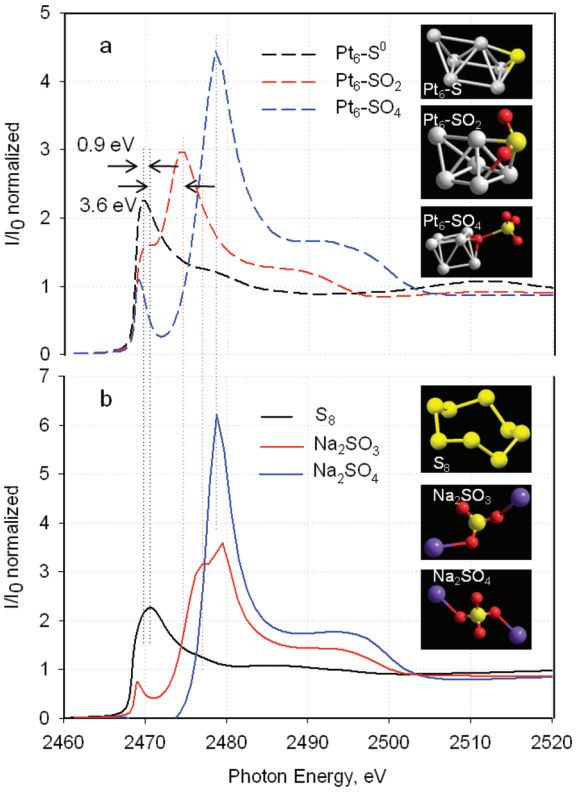

Figure 6. Simulated XANES spectra for SO_x species (x = 0, 2, and 4) adsorbed on a Pt_6 Janin cluster (a) and S_8, Na_2SO_3, and Na_2SO_4 clusters (b). Structures of the clusters used in FEFF8 modeling are shown at right.

standards, presented in Figure 2. In particular, the absorption maxima move to higher energies for S_8 (black line in Figure 6 b) and Na_2SO_4 (blue line in Figure 6 b), and their intensities increase with the sulfur oxidation state. The difference between peak positions for S_8 and Na_2SO_4 simulated spectra in Figure 6 b agrees fairly well with that for experimental curves shown in Figure 2 (8.2 eV vs 9.8 ± 0.2 eV, respectively). Although the theory describes well the shape of the single peaks for S_8 and Na_2SO_4 standards, it fails to predict the correct shape of the spectrum at 2478−2482 eV for Na_2SO_3. Instead of three peaks, the theory predicts only two peaks that are not shifted very far from the Na_2SO_4 peak. The fact that the FEFF8 model for Na_2SO_3 does not shift the main peak very far from the sulfate model indicates that there are probably issues with the Na_2SO_3 model accounting for charge transfer. There is also uncertainty in the specific physical/electronic structure for sulfites/bisulfates in general, which makes them challenging to model. Another artifact of the Na_2SO_3 model is a lower energy peak at 2469 eV that is not observed in the current experimental Na_2SO_3 spectrum or in previously published measurements.

Spectra for SO_x (x = 0, 2, and 4) species adsorbed on Pt_6 clusters (Figure 6 a) are characterized by well-pronounced maxima and pre-edge features with maxima at 2469 and 2470 eV for Pt_6-SO_2 and Pt_6-SO_4 clusters, respectively. These pre-edge features may be due to mixing Pt d orbitals with SO_x (x = 2, 4) orbitals resulting in 1s → 5d transitions. Pre-edge features are usually observed as sharp narrow peaks for platinum complexes with inorganic ligands, such as chloride.[45] These peaks are assigned to specific platinum−ligand bonding in such molecules. The question is whether these predicted features in Figure 6 a are real or are they artifacts of the modeling resulting from the small size of the Pt_6 clusters that were used for simplicity. In much bigger clusters (~3 nm, ~200 Pt atoms) like those in real Pt/VC catalysts, this peak may get broadened, so that it will become nearly invisible in the experimental XANES spectrum.

Comparison of S_8 simulated spectrum to that of Pt_6-S^0 demonstrates a −0.9 eV shift in the peak position, which is in very good agreement with −0.8 ± 0.2 eV observed as a difference between maximum on experimental S_8 spectrum and the first peak on the spectrum measured after exposure of Pt/VC catalysts to SO_2/N_2 while holding WE at 0.1 V (see Table 1). Furthermore, the difference in peak positions for S_8 and Pt_6-SO_2 models is −3.9 eV versus that of −3.6 ± 0.2 eV for the experimental S_8 spectrum and the second peak on the XANES spectrum measured after exposure to SO_2/N_2 at 0.5 and 0.7 V (see Table 1). This confirms that SO_2 adsorption product at 0.1 V is sulfur adatoms, while both sulfur adatoms and adsorbed SO_2 molecules are present on the surface of platinum nanoparticles held at 0.5 and 0.7 V. Another important point is that the first peak at 2471 ± 0.2 eV on experimental XANES spectra measured after exposure to SO_2/N_2 at 0.5 and 0.7 V may not be completely due to adsorbed sulfur atoms, but also due to SO_2 adsorbed on Pt, as a pre-edge was predicted in the simulated Pt_6-SO_2 spectrum in the same region of photon energies as the S_8 peak. The contribution of pre-edge to the first peak of XANES spectra measured after exposure to SO_2/N_2 at 0.5 and 0.7 V may also explain the 0.6 eV difference in the peak positions for the spectra measured at WEs held at 0.1 V versus 0.5 and 0.7 V (Table 1).

Regarding adsorption of sulfate ions on Pt clusters, the model does not predict a shift in the absorption maximum for the Pt_6-SO_4 versus Na_2SO_4 standard. It justifies the intuitive assumption above that the peak position of the sulfate standard can be used to confirm the presence of sulfate ions on the platinum surface.

Using Linear Combination of Sulfur Standards to Identify the Presence of Sulfate Ions on Surface of Pt/VC Catalyst at 0.1, 0.5, and 0.7 V. When the sulfate (S^{6+}) peak on the XANES spectrum interferes with the neighboring peak from sulfonic groups in the Nafion ionomer (S^{5+}), it becomes problematic to detect the presence of a small amount of sulfate ions from the apparent shift in the peak position. Nevertheless, the presence of

dx.doi.org/10.1021/la2033466 |Langmuir 2011, 27, 14930–14939

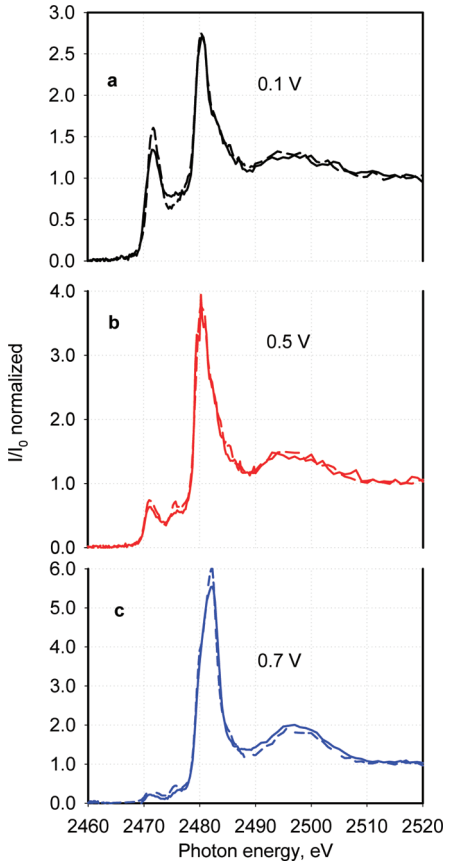

Figure 7. Experimental (—) and combination-fit (---) XANES spectra (pre-edge background corrected and normalized) for adsorbed SO_2 species on Pt/VC catalyst at 0.1 V (a), 0.5 V (b), and 0.7 V (c). See text for explanation of fitting.

sulfate ions can be qualitatively detected from the change in the shape of this peak for a mixed signal dominated by S^{5+} species. In order to verify the presence of sulfate ions on the surface at 0.1, 0.5, and 0.7 V, experimental XANES spectra were modeled by a linear combination of individual spectra for sulfur standards (S_8, Na_2SO_3, Nafion film, and diluted sulfate in carbonate), shown in Figure 2. Results of the modeling show that the shape of the main peak on experimental spectra shown in Figure 7 (—) can be simulated fairly well by linear combination of sulfur standards (---), if we assume that sulfate ions are present on the surface at 0.5 and 0.7 V, but not at 0.1 V. Coefficients obtained by curve fitting according to eq 1 are given in Table 3.

Cyclic Voltammetry after Exposure to 1000 ppm SO_2 in N_2 at 0.1−0.9 V. After recording the XANES spectra while holding the WE potential at 0.1, 0.5, and 0.7 V, a series of successive CV curves were measured starting from 0.1, 0.5, 0.7, and 0.9 V. These CV series are shown in Figure 8 a−d. SO_2 adsorption is evidenced by suppression of the hydrogen adsorption/desorption region (0.05−0.45 V) in Figure 8 a−c. The suppression of the hydrogen region becomes less pronounced as the WE hold potential increases from 0.1 to 0.9 V, implying that sulfur coverage decreases with increasing electrode potential. When the WE is held at 0.9 V during poisoning (Figure 8 d), no suppression of the hydrogen region is observed likely due to complete oxidation of SO_2 to (bi)sulfate. This assumption is consistent with the results of single cell experiments performed in

Table 3. Coefficients Obtained by Curve-Fitting Algorithm in Order to Simulate Experimental XANES Spectra by Linear Combination of Individual Spectra for S^0, S^{4+}, and S^{6+} Standards and S^{5+} from Nafion Sulfonic Group

	A (S^0)	B (S^{4+})	C (S^{5+})	D (S^{6+})
0.1 V	0.63 ± 0.01		0.37 ± 0.01	
0.5 V	0.30 ± 0.01	0.08 ± 0.01	0.57 ± 0.01	0.05 ± 0.01
0.7 V	0.12 ± 0.01	0.07 ± 0.02	0.39 ± 0.01	0.42 ± 0.01

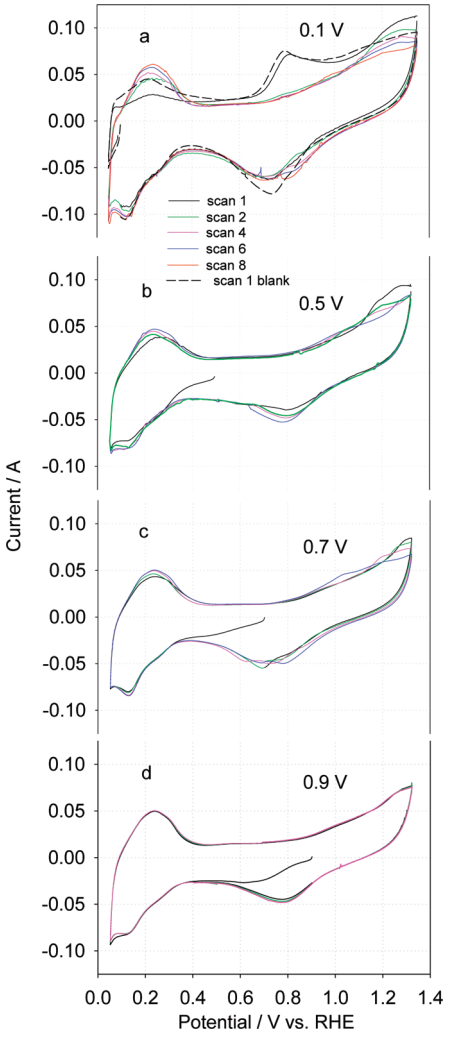

Figure 8. Series of successive CV curves recorded at 20 mV/s after measuring XANES spectra shown in Figure 4 or 5 starting from hold potentials of 0.1 (a), 0.5 (b), 0.7 (c), and 0.9 V (d). Black dashed curve in Figure 6a represents the first CV measured in a blank experiment.

$H_2|N_2$ mode.[1,9] Complete oxidation of SO_2 to (bi)sulfate ions at 0.9 V seems to contradict an experimental observation that FC suffers from SO_2 poisoning after holding the FC cathode at OCV for a few seconds. This contradiction can be easily resolved if SO_2 in air is introduced under constant cell voltage of 0.9 V instead of OCV.

The CV series shown in Figure 8 a features a broad oxidation peak at 0.885 V during the first positive-going sweep from 0.05 to 1.4 V. This peak disappears during the second positive-going sweep, and the set of following six CV curves is reminiscent of CV

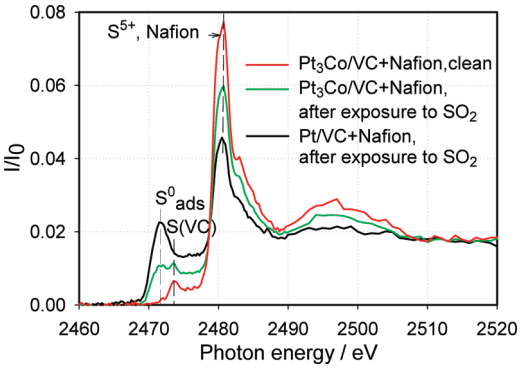

Figure 9. Pre-edge background corrected XANES spectra measured before (red) and after (green) exposure of the Pt_3Co/VC-based electrode held at 0.1 V to 1000 ppm SO_2 in N_2. Spectrum of the Pt/VC-based electrode measured after exposure to 1000 ppm SO_2 in N_2 under the same conditions (black) is shown as a reference.

series observed during oxidative sulfur desorption from the platinum surface.[1,2,46,47] The equation for this reaction was proposed by Loucka:[2]

$$Pt - S_{ads} + 4H_2O \rightarrow SO_4^{2-} + 8H^+ + 6e^- + Pt \qquad (2)$$

To confirm that adsorbed sulfur species can be completely removed from the platinum surface by successive potential cycling, a XANES spectrum (green line in Figure 4 b) was recorded after running the eight successive CV curves shown in Figure 8 b. No features are observed at 2470−2478 eV on the spectra depicted in Figure 4 b, meaning that adsorbed sulfur adatoms and SO_2 species are completely oxidized to (bi)sulfate ions. The generation of (bi)sulfate ions on the surface is confirmed by a positive 0.7 eV shift of the peak at 2480.4 eV assigned to S^{x+} from Nafion sulfonic groups (red solid and dotted curves).

The presence of the additional oxidation peak at 0.885 V in Figure 8a implies that both adsorbed sulfur and some other species are present on the platinum surface after exposure of the Pt/VC catalyst to SO_2/N_2 at 0.1 V. While "other" species are oxidized during the first oxidation sweep, sulfur still remains on the Pt surface until it is removed during successive CV sweeps by oxidation to (bi)sulfate. The other species do not originate from the SO_2/N_2 mixture, but from the research grade N_2. The black dashed line in Figure 8 a shows the first CV in the series of three measured in a blank experiment (i.e., after exposure of the WE to humidified N_2 at 0.1 V). Interestingly, both the suppression of the hydrogen region and the oxidation peak at 0.885 V were almost identical to that observed in the presence of SO_2 as observed in this blank experiment. The feature at 0.885 V is thus assigned to the oxidation of organic impurities adsorbed at 0.1 V from the research grade N_2. This organic impurity is most likely diethyl phthalate as determined by gas chromatography coupled with mass spectrometry.

Sulfur-induced reconstruction of the platinum surface resulting in an increase in the number of (100) sites was reported for polycrystalline platinum electrodes that were allowed to sit before CV was performed.[6] This seems unlikely in our experiments, because no new features were observed on the CV curve measured after SO_2 removal versus clean Pt surface for thin films of 50% Pt/VC in electrochemical cell for similar sulfur coverages and exposure times.[48]

Table 4. Peak Positions from XANES Spectra Recorded after Exposure to 1000 ppm SO_2/N_2 of the Pt_3Co/VC-Based Electrodes Held at 0.1 V

	clean CCM	0.1 V
1st peak, ±0.2 eV		2471.6
2nd peak, ±0.2 eV	2473.6	2473.5
3rd peak, ±0.2 eV	2480.6	2480.6

SO_2 Adsorption on Pt_3Co/VC versus Pt/VC Electrodes at 0.1 V: XANES. Because sulfur adatoms are the only product of SO_2 adsorption at 0.1 V, sulfur K-edge XANES can be used to distinguish between Pt_3Co and Pt nanoscale catalysts in terms of Pt−sulfur electronic interactions. These results will complement our insights on the matter obtained from electrochemical experiments both in the electrochemical cell and in the fuel cell.[14,18,19]

Cobalt atoms in the Pt_3Co alloy tune the platinum's electronic properties[49,50] in such a way that electron donation from platinum to sulfur may be expected to be less pronounced for Pt_3Co versus Pt. This was predicted for $Pt_3Co(111)$ versus Pt(111) single crystal surfaces in the presence of sulfur adatoms using density functional theory (DFT) analysis.[20] If a similar electronic effect exists for adsorbed sulfur adatoms on Pt_3Co versus Pt nanoparticles, then more pronounced electron donation from platinum to sulfur for pure platinum should result in more negative charge residing on the sulfur adatoms. A more negative charge residing on the sulfur adatoms can be identified by a negative shift in the photon energy at which the S^0 peak is observed.

XANES spectra measured on Pt_3Co/VC- and Pt/VC-based electrodes (green and black curves, respectively) after exposure to SO_2/N_2 at 0.1 V are shown in Figure 9. The reference spectrum (red line) refers to an alloy-based electrode held at 0.1 V before exposure to SO_2/N_2. The spectrum of Pt_3Co/VC catalyst is characterized by three peaks observed at 2471.6 ± 0.2, 2473.5 ± 0.2, and 2480.6 ± 0.2 eV (Table 4). The first and the last peaks are aligned with corresponding peaks on the XANES spectrum measured for SO_2 adsorbed on the Pt/VC catalyst (black line). These peaks are assigned to S^0 species and S^{5+} from the Nafion sulfonic groups above. The identical position in photon energy of the S^0 peak for Pt_3Co/VC versus Pt/VC suggests that the oxidation state of the adsorbed sulfur species is the same on both catalysts. The peak observed at 2473.5 eV is assigned to a sulfur species present in the Vulcan carbon, as it aligns well with the peak observed on the reference spectrum measured before exposure of the Pt_3Co/VC catalyst to SO_2/N_2. The reason this peak is seen on a reference spectrum measured on Pt_3Co/VC catalyst and is not seen on Pt/VC catalyst (dotted lines in Figure 4) is that the platinum loading is higher for the latter catalyst, i.e., 30 wt % Pt_3Co/VC versus 50 wt % Pt/VC catalysts. Higher platinum loading on VC for 50 wt % Pt/VC catalyst resulted in a higher platinum-to-carbon ratio in the surface layer exposed to X-rays for Pt/VC versus Pt_3Co/VC catalyst and a lower contribution from VC in the total signal.

The identical positions of the adsorption edge maxima of S^0 for Pt_3Co/VC versus Pt/VC catalysts indicate that there is no difference between the two catalysts in terms of platinum−sulfur electronic interactions. This is consistent with the results of experiments performed in an electrochemical cell.[18] Two catalysts of the same electrochemical surface area, exposed to the

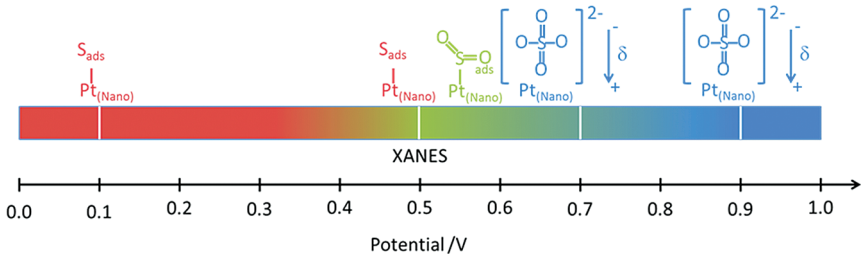

Figure 10. Comparison of sulfur speciation on Pt/VC by XANES in the potential range 0.1−0.9 V.

same SO_2 dosage, did not reveal any difference with respect to both onset potential for sulfur oxidation and sulfur coverage (see Figure 12 in ref 18). However, more detailed investigation in a broader range of sulfur coverages would be necessary to establish relationship between the results of electrochemical and XANES experiments, as comparison of Pt_3Co/VC and Pt/VC catalysts with respect to SO_2 contamination was performed only for a low sulfur coverage of 0.2 ± 0.02 (from coulometry[6]) in ref 18. More detailed discussion on the difference between the two catalysts with respect to the SO_2 contamination and recovery can be found in ref 18.

CONCLUSIONS

(1) SO_2 adsorption on commercial catalyst coated membranes employing 50 wt % Pt/VC catalyst is studied by a combination of electrochemical (potentiostatic and CV) and XANES techniques at 0.1, 0.5, 0.7, and 0.9 V in order to determine the products of SO_2 adsorption at different electrode potentials. S^0 is identified as the SO_2 adsorption product at 0.1 V, while mixtures of different ratios of S^0, SO_2, and (bi)sulfate ions are suggested at 0.5 and 0.7 V. At 0.9 V, only (bi)sulfate ions are observed on the surface. Results on SO_2 speciation on Pt/VC catalysts at 0.1−0.9 V are summarized in Figure 10.

The detection of sulfur as a product of SO_2 adsorption on platinum nanoparticles at 0.5−0.7 V (along with SO_2 and (bi)sulfate) is not consistent with what has been reported by Wilke et al.[8] for SO_2 adsorbed at the electrode/solution interface. SO_2 adsorption products were assigned in their work to two species (molecular SO_2 and SO_3 and/or sulfate) instead of three species identified in our research. This inconsistency may result from the higher reactivity of nanoparticles with respect to polycrystalline platinum due to the presence of corner and edge sites on the surface of nanoparticles. On the other hand, XANES in combination with the combination fit modeling eliminated uncertainty with respect to speciation of S^{6+} species in favor of (bi)sulfate ions (not SO_3 species) as stable products of SO_2 oxidation.

Contrary to the results of *in situ* FTIR experiments,[11,12] XANES can conclusively identify sulfur adatoms as the products of SO_2 reduction at 0.1−0.7 V. Being IR-inactive, atomic sulfur is "invisible" by FTIR. To get a complete picture of SO_2 adsorption on Pt nanoparticles, it would be interesting to compare the results on SO_2 speciation obtained by analysis of sulfur K-edge and Pt L_3-edge.[14] However, SO_2 adsorption was carried out at different conditions in these experiments (*in situ* vs *ex situ*[14]). Thus, no valid comparison can be made.

Note that the identity of adsorbed SO_2 species might change in the more oxidative environment of the fuel cell cathode. The speciation of adsorbed SO_2 species in the presence of molecular oxygen has been recently determined in X-ray absorption experiments similar to those performed in SO_2/N_2. The publication of these results is under way.

(2) Sulfur speciation is verified by modeling of XANES spectra for SO_x (x = 0, 2, and 4) species adsorbed on Pt_6 Janin cluster versus clusters of sulfur standards (S_8, Na_2SO_3, and Na_2SO_4). A good agreement is observed between experiment and the theory with respect to shifts in peak positions for Pt_6−S and Pt_6−SO_2 clusters versus S_8 clusters. Modeling confirms that no shift in peak position is observed for SO_4^{2-} species adsorbed on platinum versus Na_2SO_4 cluster, which is consistent with significant weakening of platinum−sulfur interaction when these atoms are separated by oxygen atoms. Theory predicts pre-edge features at 2469 eV for SO_x (x = 2 and 4) species adsorbed on Pt that may affect the shape of the peak assigned to sulfur adatoms if the mixture of adsorbed SO_x (x = 0, 2, and 4) species is present on the Pt surface.

Although FEFF8 modeling is frequently used to model adsorbed species on platinum clusters, raw spectra are not very frequently reported and compared with experimental spectra. We demonstrate here that such comparison may provide a valuable insight into the origin of some features observed in the experimental spectra. For the first time we have shown that FEFF8 modeling can be successfully used to quantitatively interpret the shifts in absorption maxima caused by metal−adsorbate interactions.

(3) XANES is used to compare Pt_3Co/VC and Pt/VC catalysts in terms of platinum−sulfur electronic interactions. In agreement with electrochemical experiments,[18] there is no detectable difference between the two catalysts in terms of platinum−sulfur electronic interactions.

AUTHOR INFORMATION

Corresponding Author

*Phone:1-202-767-6345. E-mail: olga.baturina@nrl.navy.mil.

ACKNOWLEDGMENT

The authors are grateful to the Office of Naval Research for financial support of this project. We also thank Dr. Karen Swider-Lyons from the Naval Research Laboratory and Professor D. Ramaker from George Washington University for helpful suggestions when discussing this paper. Beamline X15B is supported and operated by a multi-institutional consortium of scientists coordinated by Stony Brook University. The National Synchrotron Light Source is supported by the Department of Energy.

REFERENCES

(1) Baturina, O. A.; Swider-Lyons, K. E. *J. Electrochem. Soc.* **2009**, *156*, B1423–B1430.

(2) Loucka, T. *J. Electroanal. Chem.* **1971**, *31*, 319–332.

(3) Matveeva, E. S.; Shepelin, V. A.; Kasatkin, E. V. *Elektrokhimiya* **1982**, *18*, 634–636.
(4) Matveeva, E. S.; Shepelin, V. A.; Kasatkin, E. V. *Elektrokhimiya* **1981**, *17*, 617–620.
(5) Szklarczyk, M.; Czerwinski, A.; Sobkowski, J. *J. Electroanal. Chem.* **1982**, *132*, 263–271.
(6) Foral, M. J.; Langer, S. H. *J. Electroanal. Chem.* **1988**, *246*, 193–205.
(7) Quijada, C.; Vazquez, J. L.; Perez, J. M.; Aldaz, A. *J. Electroanal. Chem.* **1994**, *372*, 243–250.
(8) Wilke, T.; Gao, X. P.; Takoudis, C. G.; Weaver, M. J. *J. Catal.* **1991**, *130*, 62–75.
(9) Nagahara, Y.; Sugawara, S.; Shinohara, K. *J. Power Sources* **2008**, *182*, 422–428.
(10) Fu, J.; Hou, M.; Du, C.; Shao, Z.; Yi, B. *J. Power Sources* **2009**, *187*, 32–38.
(11) Quijada, C.; Rodes, A.; Vazquez, J. L.; Perez, J. M.; Aldaz, A. *J. Electroanal. Chem.* **1995**, *398*, 105–115.
(12) Quijada, C.; Rodes, A.; Vazquez, J. L.; Perez, J. M.; Aldaz, A. *J. Electroanal. Chem.* **1995**, *394*, 217–227.
(13) Rodriguez, J. A.; Wang, X.; Liu, G.; Hansona, J. C.; Hrbek, J.; Peden, C. H. F.; Iglesias-Juez, A.; Fernandez-Garcia, M. *J. Mol. Catal. A: Chem.* **2005**, *228*, 11–19.
(14) Ramaker, D. E.; Gatewood, D.; Korovina, A.; Garsany, Y.; Swider-Lyons, K. E. *J. Phys. Chem. C* **2010**, *114*, 11886–11897.
(15) Frank, P.; George, S. D.; Anxolabehere-Mallart, E.; Hedman, B.; Hodgson, K. O. *Inorg. Chem.* **2006**, *45*, 9864–9876.
(16) Ankudinov, A. L.; Ravel, B.; Rehr, J. J.; Conradson, S. D. *Phys. Rev. B* **1998**, *58*, 7565–7576.
(17) Waldo, G. S.; Carlson, R. M. K.; Moldowan, J. M.; Peters, K. E.; Pennerhahn, J. E. *Geochim. Cosmochim. Acta* **1991**, *55*, 801–814.
(18) Baturina, O. A.; Gould, B. D.; Garsany, Y.; Swider-Lyons, K. *Electrochim. Acta* **2010**, *55*, 6676–6686.
(19) Garsany, Y.; Baturina, O. A.; Swider-Lyons, K. E. *J. Electrochem. Soc.* **2009**, *156*, B848–B855.
(20) Pillay, D.; Johannes, M. D.; Garsany, Y.; Swider-Lyons, K. E. *J. Phys Chem. C* **2010**, *114*, 7822–7830.
(21) Sasaki, K.; Wang, J. X.; Balasubramanian, M.; McBreen, J.; Uribe, F.; Adzic, R. R. *Electrochim. Acta* **2004**, *49*, 3873–3877.
(22) http://www.nsls.bnl.gov/beamlines/beamline.asp?blid=x15b.
(23) Press, W. H.; Flannery, B. P.; Teukolsky, S. A.; Vetterling, W. T. *Numerical Recipes*; Cambridge University Press: Cambridge, U.K., 1986.
(24) Newville, M.; Livins, P.; Yacoby, Y.; Rehr, J. J.; Stern, E. A. *Phys. Rev. B* **1993**, *47*, 14126–14131.
(25) Risberg, E. D.; Eriksson, L.; Mink, J.; Pettersson, L. G. M.; Skripkin, M. Y.; Sandstrom, M. *Inorg. Chem.* **2007**, *46*, 8332–8348.
(26) Larsson, L. O.; Kierkega., P *Acta Chem. Scand.* **1969**, *23*, 2253–&.
(27) Nord, A. G. *Acta Chem. Scand.* **1973**, *27*, 814–822.
(28) Villars, P.; Calvert, L. *Pearson's Handbook of Crystallographic Data for Intermetallic Phases*, 2nd ed.; ASM International: Materials Park, OH, 1991.
(29) Janin, E.; von Schenck, H.; Gothelid, M.; Karlsson, U. O.; Svensson, M. *Phys. Rev. B* **2000**, *61*, 13144–13149.
(30) Ankudinov, A. L.; Rehr, J. J.; Low, J.; Bare, S. R. *Phys. Rev. Lett.* **2001**, *86*, 1642–1645.
(31) Ankudinov, A. L.; Rehr, J. J.; Low, J. J.; Bare, S. R. *J. Chem. Phys.* **2002**, *116*, 1911–1919.
(32) Lin, X.; Hass, K. C.; Schneider, W. F.; Trout, B. L. *J. Phys. Chem. B* **2002**, *106*, 12575–12583.
(33) Lin, X.; Schneider, W. F.; Trout, B. L. *J. Phys. Chem. B* **2004**, *108*, 250–264.
(34) Lin, X.; Schneider, W. F.; Trout, B. L. *J. Phys. Chem. B* **2004**, *108*, 13329–13340.
(35) Vairavamurthy, A. *Spectrochim. Acta, Part A* **1998**, *54*, 2009–2017.
(36) Einsiedl, F.; Schafer, T.; Northrup, P. *Chem. Geol.* **2007**, *238*, 268–276.
(37) Solomon, D.; Lehmann, J.; Martinez, C. E. *Soil Sci. Soc. Am. J.* **2003**, *67*, 1721–1731.
(38) Xia, K.; Weesner, F.; Bleam, W. F.; Bloom, P. R.; Skyllberg, U. L.; Helmke, P. A. *Soil Sci. Soc. Am. J.* **1998**, *62*, 1240–1246.
(39) HeitnerWirguin, C. *J. Membr. Sci.* **1996**, *120*, 1–33.
(40) Spotnitz, R. M.; Colucci, J. A.; Langer, S. H. *Electrochim. Acta* **1983**, *28*, 1053–1062.
(41) Swider, E. E.; Rolison, D. R. *Langmuir* **1999**, *15*, 3302–3306.
(42) Thomas, S.; Sung, Y. E.; Kim, H. S.; Wieckowski, A. *J. Phys. Chem.* **1996**, *100*, 11726–11735.
(43) Kunimatsu, K.; Samant, M. G.; Seki, H. *J. Electroanal. Chem.* **1989**, *258*, 163–177.
(44) Tebbe, F. N.; Wasserman, E.; Peet, W. G.; Vatvars, A.; Hayman, A. C. *J. Am. Chem. Soc.* **1982**, *104*, 4971–4972.
(45) Sugiura, C.; Muramatsu, S. *J. Phys. Chem. Solids* **1985**, *46*, 1215–1219.
(46) Garsany, Y.; Baturina, O. A.; Swider-Lyons, K. E. *J. Electrochem. Soc.* **2007**, *154*, B670–B675.
(47) Gould, B. D.; Baturina, O. A.; Swider-Lyons, K. E. *J. Power Sources* **2009**, *188*, 89–95.
(48) Baturina, O. A.; Gould, B. D.; Garsany, Y.; Swider-Lyons, K. E. *Electrochim. Acta* **2010**, *55*, 6676–6686.
(49) Stamenkovic, V. R.; Mun, B. S.; Mayrhofer, K. J. J.; Ross, P. N.; Markovic, N. M. *J. Am. Chem. Soc.* **2006**, *128*, 8813–8819.
(50) Duong, H. T.; Rigsby, M. A.; Zhou, W.-P.; Wieckowski, A. *J. Phys. Chem. C* **2007**, *111*, 13460–13465.